WM2008 Conference, February 24 -28, 2008, Phoenix, AZ
Abstract #8438

Thermodynamic Properties of Actinide-Zirconium Dioxide Solid-Solutions Relevant for Advanced Nuclear Fuels

L.C. Shuller[1], N. Pavenayotin[2], F.N. Skomurski[3], R.C. Ewing[1,2,4], U. Becker[4]

[1]Materials Science and Engineering Department, University of Michigan; [2]Nuclear Engineering and Radiological Sciences Department, University of Michigan; [3]EMSL, Pacific Northwest National Laboratory; [4]Geological Sciences Department, University of Michigan

ABSTRACT

Currently, spent nuclear fuel (SNF) from commercial reactors is composed of 95-99% UO_2 and 1-5% fission products and transuranium elements. Thus, the primary waste form is the UO_2 matrix, which over time will corrode to a variety of U(VI)-secondary phases. Alternative nuclear fuels, such as inert-matrix fuels and mixed-oxide fuels, have been studied for their in-reactor performance; however little research has been conducted to understand the behavior of these fuels as a wasteform. We use density functional theory and Monte-Carlo methods to understand the solid solution behavior of (Ac, Zr)O_2 (Ac = Th, U, Np, Pu) phases. The end members of interest include ZrO_2, ThO_2, UO_2, NpO_2, and PuO_2, and all share the cubic-flourite structure. The excess enthalpy of mixing (ΔH_{excess}), excess Gibbs free energy of mixing (ΔG_{excess}), and excess configurational entropy (ΔS_{excess}) are calculated for the above solid solution series, and from ΔG_{excess}, miscibility gaps are identified.

INTRODUCTION

Uranium dioxide (UO_2) is the most widely used nuclear fuel material, and spent nuclear fuel is composed of approximately 95 % UO_2 and 5 % fission products and transuranium elements [1]. From a waste management standpoint, UO_2 is not the most ideal matrix since uranium has four oxidation states (3^+ through 6^+), and the solubility of uranium phases increases with increasing oxidation state [2]. UO_2 oxidizes more readily in the presence of water than under dry conditions, which can lead to the release of uranium as well as transuranic elements that are in solid solution with the UO_2 matrix. However, if Th is incorporated in solid solution of UO_2, creating a mixed-oxide fuel, the corrosion resistance of the spent fuel can be improved.

ThO_2 and ZrO_2 solid solutions are frequently used to stabilize UO_2 fuel as all compounds share the cubic fluorite structure, and ThO_2 and ZrO_2 provide increased corrosion resistance. ZrO_2 has been studied as a host material for immobilization of actinides. It is a good candidate for waste form because of its ability to incorporate actinides into its structure [3]. Like U-238, Th-232 is a fertile nuclear material, so it can be used as a nuclear fuel in conjunction with a fissile counterpart. Unlike U, Th has only one oxidation state of 4^+ and no unpaired electrons. As a result, ThO_2 is an insulator. These properties combined contribute to the greater corrosion resistance of ThO_2 as compared with UO_2 [4, 5].

During burn-up in the reactor, fission products and long-lived actinides are also produced. The common actinides found in spent nuclear fuels are Np, Pu, Am, and Cm. The oxides of these actinides also have the fluorite structure. Since these elements form solid solutions with the UO_2 matrix, it is important to understand their limits of incorporation and the degree to which they can be retained by the spent fuel matrix to prevent their release into the environment.

In this study, the thermodynamic properties of binary solid solutions of AcO_2 (Ac = Th, U, Np, Pu) and ZrO_2 are examined using computational techniques. Density functional theory (DFT)

methods were used to determine the excess enthalpies of mixing for each series (ΔH_{excess}). Monte-Carlo methods were used to calculate excess Gibbs free energy of mixing (ΔG_{excess}), and excess configurational entropy (ΔS_{excess}). From these results, the miscibility of these solid solution series is determined which has application for understanding the stability of mixed-oxide or inert-matrix fuels as a waste form.

METHODS

Two computational techniques were used in this study to determine the solid solution thermodynamic properties: 1) *ab initio* geometry optimizations and 2) Monte-Carlo simulations. The *ab initio* calculations were conducted for several binary oxide solid solution series to determine the optimized geometry of the end members (e.g., ZrO_2, ThO_2), as well as intermediate members (e.g., $Th_{0.5}Zr_{0.5}O_2$). The excess enthalpy of mixing for each solid solution series was calculated from the *ab initio* results, where each system is in its ground state (temperature = 0 K). The final energies from the *ab initio* calculations are then used to calculate cation-cation interaction parameters for all possible pairs of exchangeable cations. For instance, in the $Th_{1-x}Zr_xO_2$ series, interaction parameters are calculated for Th-Zr, Th-Th, and Zr-Zr. The interaction parameters are then used in the Monte-Carlo simulation to calculate thermodynamic properties of the solid solution series, specifically the excess enthalpy, excess free energy, and excess entropy of mixing as a function of temperature. Using such a Monte-Carlo approach allows one to evaluate millions of configurations for different compositions in much larger supercells than possible using only an *ab-initio* procedure.

Ab initio calculations

The program CASTEP (CAmbridge Serial Total Energy Package) [6] was used for the geometry optimizations and ground state total energy calculations. CASTEP is a density functional theory-based code that uses plane waves as the basis function and pseudo-potentials to approximate the behavior of the core electrons. Ultra-soft pseudopotentials were used, which include relativistic effects. The spin-polarized generalized gradient approximation (GGA) with the PW-91 [7] functional was used to approximate the valence electron exchange and correlation interactions. The kinetic energy cut-off for the planewaves was chosen to be 800 eV and the k-point spacing was 0.1 $Å^{-1}$. The total energy convergence tolerance was $9 \cdot 10^{-5}$ eV/atom.

The four binary oxides of interest for advanced nuclear fuels include ZrO_2, ThO_2, UO_2, and PuO_2. Therefore, the four solid solution series include $Th_{1-x}Zr_xO_2$, $U_{1-x}Zr_xO_2$, $Np_{1-x}Zr_xO_2$, and $Pu_{1-x}Zr_xO_2$. All of the binary oxides have the cubic fluorite structure, and each unit cell contains four formula units (Z=4), resulting in four possible exchangeable cation sites. The *ab initio* calculations were conducted for compositions of $A_{1-x}B_xO_2$, where x = 0.00, 0.25, 0.50, 0.75, and 1.00. For geometry optimizations of the unit cells, *P1* symmetry was imposed and the starting lattice parameters for the intermediate structures were weighted averages of the end member lattice parameters. A spin-polarized approach was used for unit cells containing U, Np, or Pu to take into account the behavior of the unpaired 5f electrons in the 4+ oxidation state of each element, for which there are 2, 3, and 4 unpaired 5f electrons, respectively.

Generating interaction parameters

The total energy of a system calculated in CASTEP is the formation energy from the zero valent gaseous species (Equation 1). The energy of mixing of cation A into BO_2 is described by a Hamiltonian that takes into account the interactions between the cations (Equation 2).

$$(1\text{-}x)A^0 + xB^0 + 2O^0 \rightarrow A_{(1-x)}B_xO_2 \quad (1)$$

$$E_{excess} = E_0 + \sum(n^i_{A\text{-}B}E^i_{A\text{-}B} + n^i_{A\text{-}A}E^i_{A\text{-}A} + n^i_{B\text{-}B}E^i_{B\text{-}B}) \quad (2)$$

In Equation 2, i is the interaction type as described by the distance of the cation interaction, n^i is the number of iterations of a type in a given cell configuration, and E^i is the energy of forming the given cation-cation pair. With E_0, we describe the asymmetry of the system as approximated by a Margules function $E_0 = x(1\text{-}x)$ [(xW.(1-x)W)]. The Margules parameter W is also listed in Table I. Due to the computational expense of the *ab initio* calculations, cell configurations were limited to 1×1×1 unit cells. Therefore, the one interaction type for the cubic $A_{(1-x)}B_xO_2$ cell is the nearest neighbor interaction. Later calculations are concerned with excess properties, so the interaction energies from Equation 2 (E^i) are combined into an exchange parameter J^i, which describes the energy associated with the A-B cation exchange (Equation 3).

$$J^i_{A\text{-}B} = E^i_{A\text{-}B} - \tfrac{1}{2}(E^i_{A\text{-}A} + E^i_{B\text{-}B}) \quad (3)$$

The $J^i_{A\text{-}B}$ is fit to the excess energy of mixing that was derived quantum mechanically for the solid solution series according to Equation 4.

$$E_{excess} = E_0 + \sum n^i_{A\text{-}B}J^i_{A\text{-}B} \quad (4)$$

The exchange parameters for the solid solution series are listed in Table I.

Table I. Margules Parameters (W_1, W_2) and Exchange Parameters ($J^i_{A\text{-}B}$) for the Binary Oxide Solid Solution Series Fit to Excess Energies Calculated Using CASTEP.

Solid Solution $A_{1-x}B_xO_2$	W [kJ/mol]	$J^i_{A\text{-}B}$ [kJ/(mol interactions)]
$Th_{1-x}Zr_xO_2$	29.6	0.66101
$U_{1-x}Zr_xO_2$	8.1	0.61265
$Np_{1-x}Zr_xO_2$	13.2	0.48835
$Pu_{1-x}Zr_xO_2$	21.3	0.66479

Monte-Carlo simulations

The exchange parameters J^i are used in the Monte-Carlo simulations to calculate the lattice energy for millions of different cation configurations. The excess enthalpy of mixing is calculated for the solid solution series using the methodology described by Becker *et al.* [8]. An energy E is associated with each starting configuration and the energy change associated with swapping cation positions is ΔE. If ΔE is negative, meaning that the new configuration is more energetically favorable than the starting configuration, the new configuration is accepted with a probability of one. If ΔE is positive, then the new configuration is accepted with a probability following a Boltzmann distribution. 8×8×8 supercells were constructed, resulting in 2048 exchangeable cation sites. The excess entropy and free energy of mixing are then calculated using the Bogoliubov integration scheme [9,10].

RESULTS AND DISCUSSION

Enthalpy of mixing

The excess enthalpy of mixing (ΔH_{excess}) for the binary oxide solid solutions are plotted as a function of composition X_{Zr}, which is the molar fraction of Zr/(Zr + Ac), where Ac is Th, U, Np, or Pu. For example, the excess enthalpy of mixing for the $Th_{1-x}Zr_xO_2$ solid solution series is plotted as a function of the molar fraction of Zr/(Zr+Th). The Monte Carlo data are plotted over the temperature range 100K to infinite temperature – specifically at 100K, 200K, 300K, 400K, 500K, 600K, 700K, 800K, 900K, 1000K, 1500K, 2000K, and ∞. The quantum-mechanical results are overlaid for comparison. The solid solution series do not show any favorable intermediate phases with respect to the average of the binary oxide end members. Single unit cells were used in the quantum-mechanical calculations due to limitations of the technique; therefore, only one cation-cation interaction parameter could be calculated and ordering could not be determined. Molecular dynamics simulations will be used in future calculations to correct for this limitation.

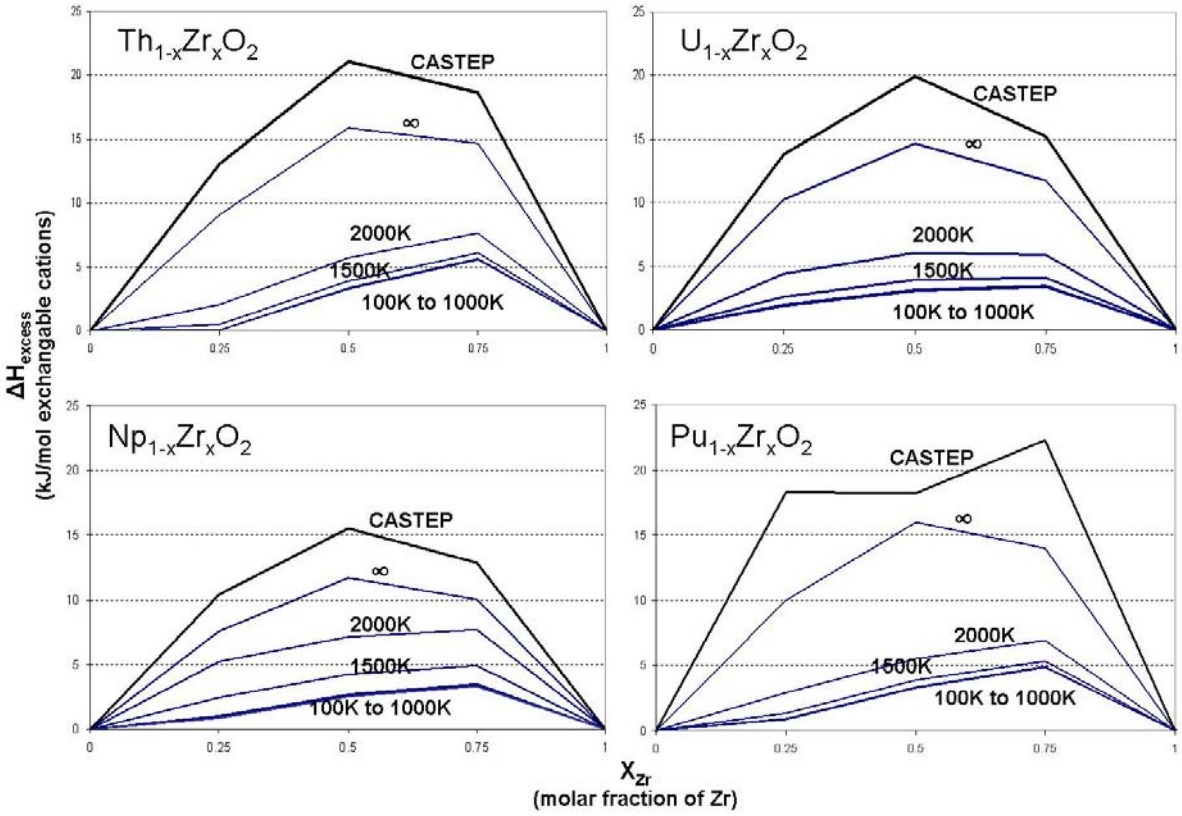

Figure 1. Excess free enthalpy of mixing (ΔH_{excess}, kJ/mol exchangeable cation) as a function of the molar fraction of Zr (X_{Zr}) for the $Th_{1-x}Zr_xO_2$, $U_{1-x}Zr_xO_2$, $Np_{1-x}Zr_xO_2$, and $Pu_{1-x}Zr_xO_2$ solid solution series. The upper-most curve is the result from the quantum-mechanical (CASTEP) calculations, while the other curves are from the Monte-Carlo simulations over a temperature range from 100K to infinite temperature (∞), calculated in increments of 100 K below 1000 K, and increments of 500 K above 1000 K.

Gibbs free energy of mixing

The excess Gibbs free energy of mixing (ΔG_{excess}) was calculated using a post-Monte Carlo Bogoliubov integration scheme. The results are shown in Figure 2. The solid solution series have similar trends. The minimum point on the ΔG_{excess} vs. composition curve indicates the composition that results in a composition that is thermodynamically stable (when the minimum occurs at negative ΔG_{excess}). At all temperatures tested, ThO_2 can incorporate limited amounts of Zr into the structure (~25%). All other series can incorporate the same amount of Zr into the AcO_2 structure, but at limited temperatures. Above 1500K, ~25% of Zr can be incorporated into the UO_2 structure. The NpO_2 structure can incorporate ~25% of Zr above 800K, and the PuO_2 structure can incorporate ~25% of Zr above 600K. Only trace amounts of the actinides are thermodynamically stable in the ZrO_2 structure.

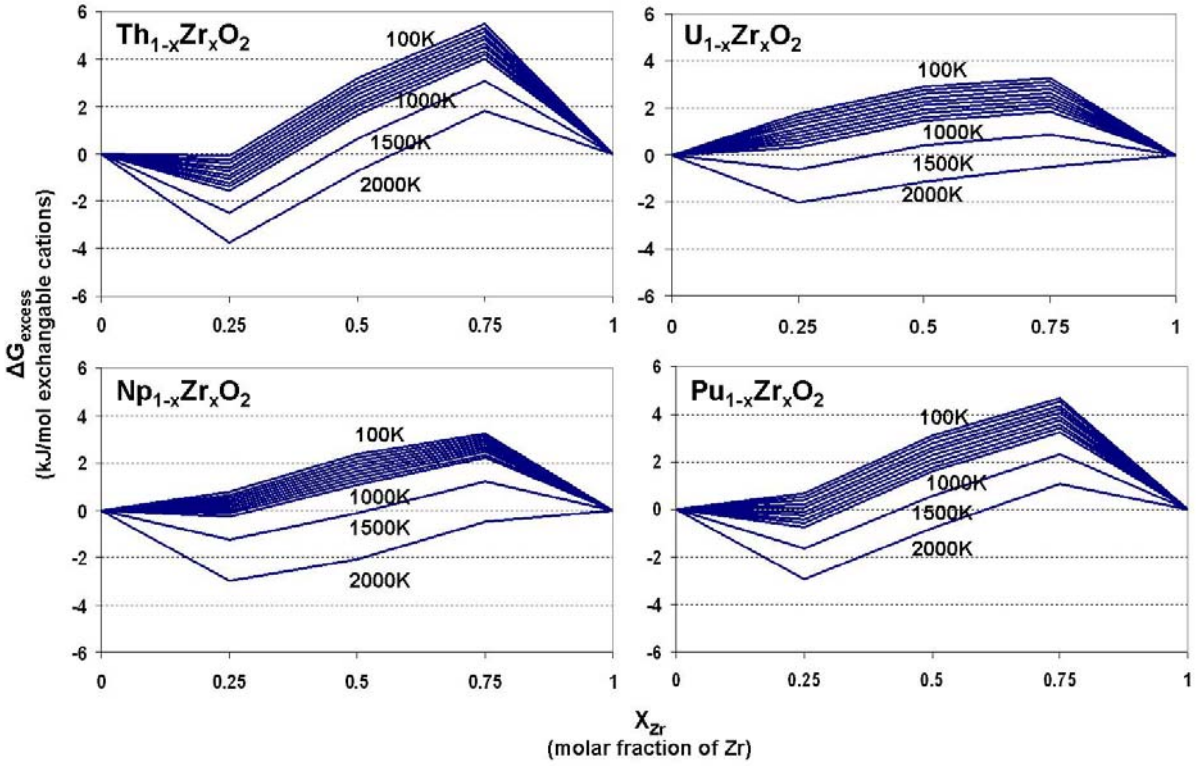

Figure 2. Excess Gibbs free energy of mixing (ΔG_{excess}, kJ/mol exchangeable cation) as a function of the molar fraction of Zr (X_{Zr}) for the $Th_{1-x}Zr_xO_2$, $U_{1-x}Zr_xO_2$, $Np_{1-x}Zr_xO_2$, and $Pu_{1-x}Zr_xO_2$ solid solution series. The Monte-Carlo simulation was calculated for the temperature range from 100K to 2000K, calculated in increments of 100 K below 1000 K, and increments of 500 K above 1000 K.

Configurational entropy

The excess configurational entropy (ΔS_{excess}) is determined from the difference between the excess enthalpy and the excess free energy (Figure 3) and by dividing this difference by (-T). The excess configurational entropy curves for the all of the solid solution series are comparable and indicate that even at T as high as 2000K the entropy is still a fraction (½ for the $Th_{1-x}Zr_xO_2$, $U_{1-x}Zr_xO_2$, and $Pu_{1-x}Zr_xO_2$ series and ¾ for the $Np_{1-x}Zr_xO_2$ series) of the point entropy, which is defined as the configurational entropy without ordering. Thus, even at such a high T, the systems are partially exsolved or cation-ordered. The point entropy is defined by Equation 5 and

is the same for all binary systems. A specific ordering scheme is not observed yet because the systems used in the initial quantum-mechanical calculations were limited to a single cubic unit cell, where all of the cation sites are symmetrically equivalent and have the same nearest-neighbors and cation-cation distances. Larger systems are necessary to consider ordering such that higher-order cation-cation interactions can be considered in addition to the next nearest neighbor interactions used in this study. Enlarging the system can be achieved with quantum-mechanical calculations; however, the time of the calculation increases by N^3, where N is the number of atoms in the system. Thus, empirical potential calculations are useful for determining the configuration of systems on the order of hundreds to thousands of atoms.

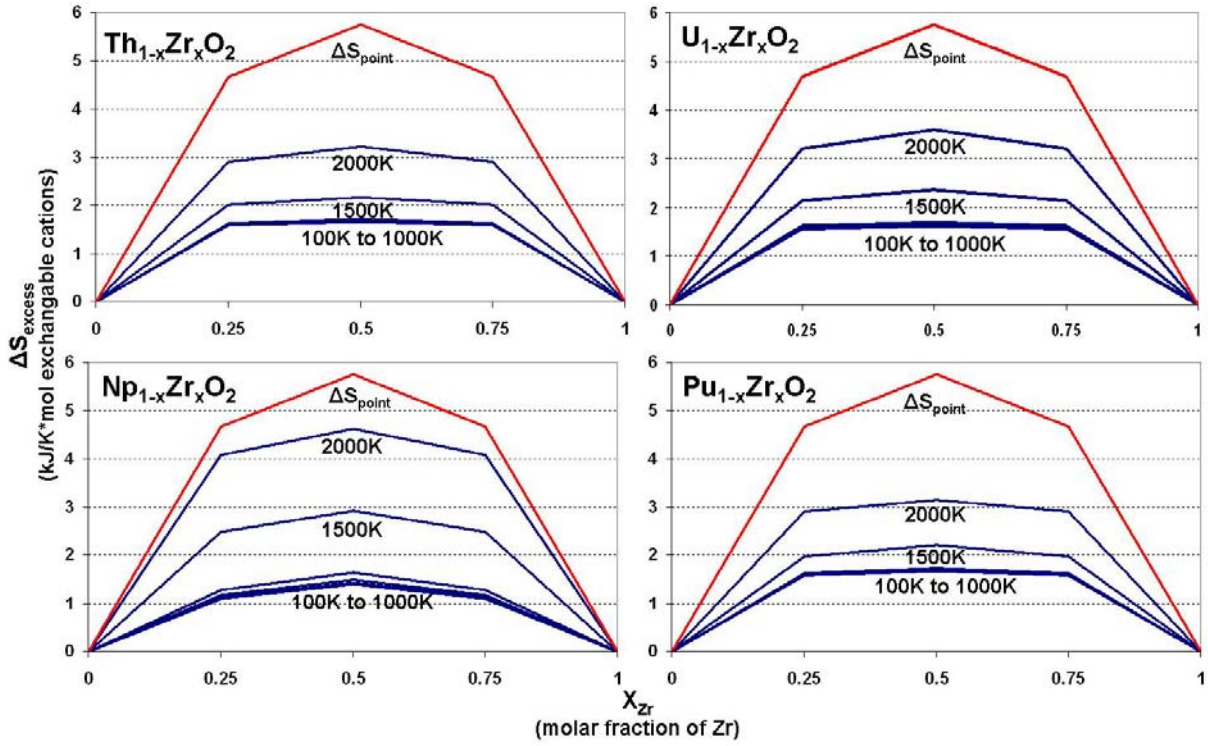

Figure 3. Excess configurational entropy (ΔS_{excess}, kJ/K*mol exchangeable cation) as a function of the molar fraction of Zr (X_{Zr}) for the $Th_{1-x}Zr_xO_2$, $U_{1-x}Zr_xO_2$, $Np_{1-x}Zr_xO_2$, and $Pu_{1-x}Zr_xO_2$ solid solution series. The arrows indicate the direction of increasing temperature from 100K to 2000K, in increments of 100 K below 1000 K, and increments of 500 K above 1000 K.

$$\Delta S_{point} = -R[X_{Zr}\ln X_{Zr} + (1-X_{Zr})\ln(1-X_{Zr})] \quad (5)$$

CONCLUSIONS

Density functional theory and Monte Carlo simulations were used in this study to determine the thermodynamic properties of binary oxide solid solutions that are useful for advanced nuclear fuel applications. The DFT results for each solid solution series is of the single cubic unit cell; therefore, only one interaction parameter was calculated. Based on the Monte-Carlo results, on the order of 25% Zr can be incorporated into the AcO_2 structures (Ac = Th, U, Np, or Pu). However, only trace amounts of the actinides can be incorporated into ZrO_2. Considering larger systems in the DFT calculations will improve results, because more cation-cation interaction parameters can be calculated. Configurational ordering can also be considered with larger

systems. Molecular dynamic simulations will be used to determine the temperature dependence of the different solid solutions that is more specific to their respective lattice dynamics.

REFERENCES

1. J. Janeczek, R.C. Ewing, V.M. Oversby, and L.O. Werme, "Uraninite and UO_2 in spent nuclear fuel: a comparison," Journal of Nuclear Materials, **238,** 121-130 (1996).
2. D.W. Shoesmith, "Fuel corrosion processes under waste disposal conditions," Journal of Nuclear Materials, **282,** 1-31 (2000).
3. R.B. Heimann, and T.T. Vandergraaf, "Cubic zirconia as a candidate waste form for actinides: Dissolution studies," Journal of Materials Science Letters, **7(6)**, 583-586 (1988).
4. G. Heisbourg, S. Hubert, N. Dacheux, and J. Purans, "Kinetic and thermodynamic studies of the dissolution of thoria-urania solid solutions," Journal of Nuclear Materials, **335**, 5-13 (2004).
5. F.N. Skomurski, L.C. Shuller, R.C. Ewing, and U. Becker, "Corrosion of UO_2 and ThO_2: A quantum mechanical investigation," Journal of Nuclear Materials, (*in press*).
6. M.D. Segall, P.J.D. Lindan, M.J. Probert, C.J. Pickard, P.J. Hasnip, S.J. Clark, and M.C. Payne, "First-principles simulation: ideas, illustrations and the CASTEP code," Journal of Physics: Condensed Matter, **14(11)**, 2717-2743 (2002).
7. J.P. Perdew and Y. Wang, "Accurate and simple analytic representation of the electron-gas correlation-energy," Physical Review B, **45**, 13244-13249 (1992).
8. U. Becker, A. Fernandez-Gonzalez, M. Prieto, R. Harrison, and A. Putnis, "Direct calculation of thermodynamic properties of the barite/celestite solid solution from molecular principles," Physical Chemical Mineralogy, **27**, 291-300 (2000).
9. M. Reich and U. Becker, "First-principles calculations of the thermodynamic mixing properties of arsenic incorporation into pyrite and marcasite," Chemical Geology, **225**, 278-290 (2006).
10. J.M. Yeomans, Statistical Mechanics of Phase Transitions, Oxford Science Publications, Clarendon Press, Oxford, (1992).